Measurements of jet substructure using the CMS detector

Jelena Mijušković

on behalf of the CMS collaboration

31st International Workshop on Deep Inelastic Scattering

April 2024

Introduction

- Jet substructure - provides numerous innovative new ways to search for new physics and to probe the Standard Model in extreme regions of phase space
- Experimental precision to challenge state-of-the-art pQCD analytical calculations and to constrain parton shower & hadronization models of Monte Carlo generators

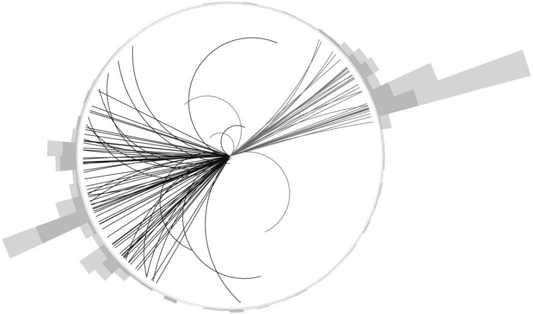

Introduction

Covered in this talk:

1. *Measurement of the primary Lund jet plane density in proton-proton collisions at $\sqrt{s}$= 13 TeV*
   CMS-SMP-22-007, Submitted to J. High Energy Phys.
2. *Measurement of energy correlators inside jets and determination of the strong coupling $\alpha_S(m_Z)$*
   CMS-SMP-22-015, Submitted to Phys. Rev. Lett.
3. *Observation of enhanced long-range elliptic anisotropies inside high-multiplicity jets in pp collisions at $\sqrt{s}$= 13 TeV*
   CMS-HIN-21-013, Submitted to Phys. Rev. Lett.
4. *Groomed jet radius and girth of jets recoiling against isolated photons in PbPb and pp collisions at 5.02 TeV*
   CMS-PAS-HIN-23-001

Lund jet plane

CMS-SMP-22-007

- Lund planes - 2D representation of the phase-space of 1→2 splittings

$$\Delta R = \sqrt{(y^{j_1} - y^{j_2})^2 + (\phi^{j_1} - \phi^{j_2})^2},$$

$$k_{\mathrm{T}} = p_{\mathrm{T}}^{j_2} \Delta R$$

- Internal structure of the jet - **iterative jet declustering** using the Cambridge–Aachen (CA) algorithm
- **Primary Lund jet plane** - emissions obtained by declustering the harder subjet at each step of the declustering process
- Provides information about the radiation pattern of the jet

Measurement of PLJP density, directly proportional to α_S:

$$\frac{1}{N_{\text{jets}}} \frac{d^2 N_{\text{emissions}}}{d\ln(k_T) d\ln(R/\Delta R)} = \frac{2}{\pi} C_R \alpha_s(k_T)$$

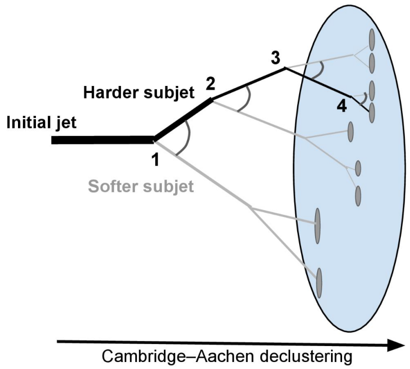

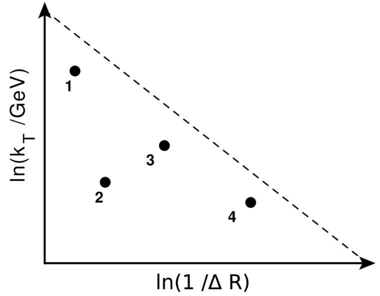

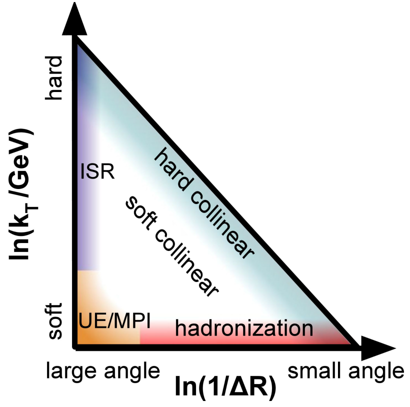

Lund jet plane

CMS-SMP-22-007

- pp data collected at $\sqrt{s}$ = 13 TeV during Run 2 (2016–2018), integrated luminosity of 138 fb^{-1}
- Anti-k_T jets with p_T^{jet} > 700 GeV and |y| < 1.7
- Charged particles of the anti-k_T jet reclustered with the CA algorithm to construct the LJP
- Two distance parameters: R = 0.4 and R = 0.8
- Distributions unfolded to particle level

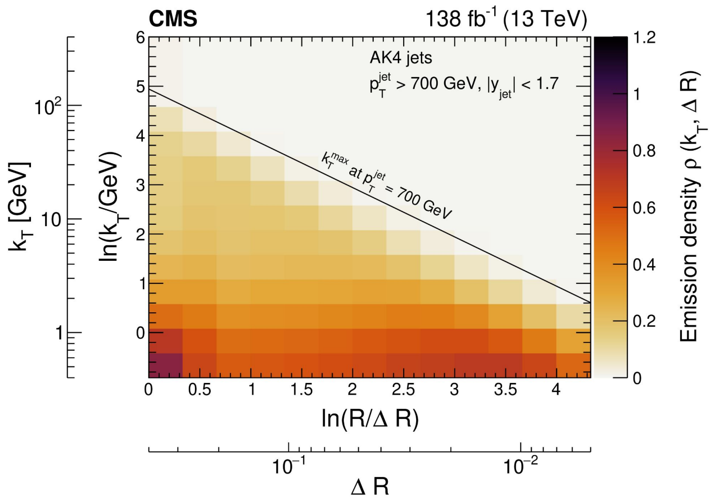

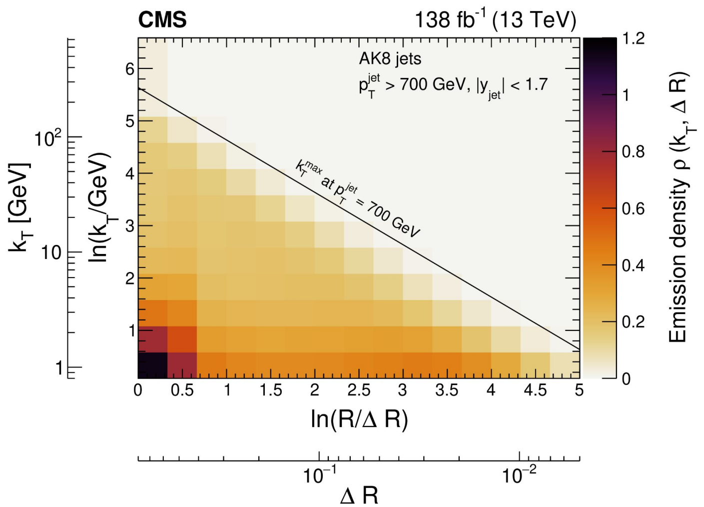

➢ LJP density approximately flat for hard and collinear emissions due to $\alpha_S(k_T) \sim 1/\ln(k_T)$

Lund jet plane

CMS-SMP-22-007

- Corrected primary LJP density compared with various particle-level predictions
  different parton showers, underlying-event activity, hadronization, and color reconnection effects

➢ **Strong constraints in terms of the substructure of jets with factorisation of these mechanism using LJP**

Low-k_T (hadronization effects and UE):

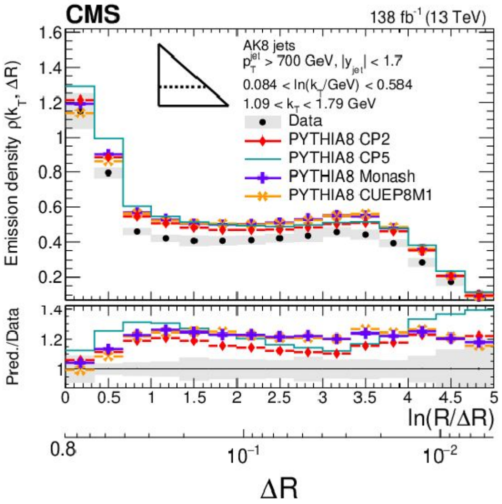

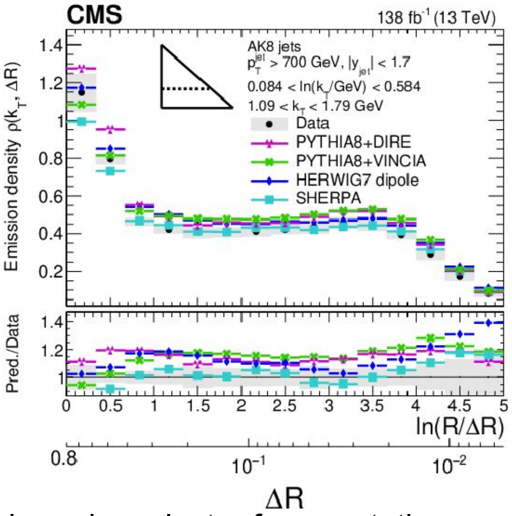

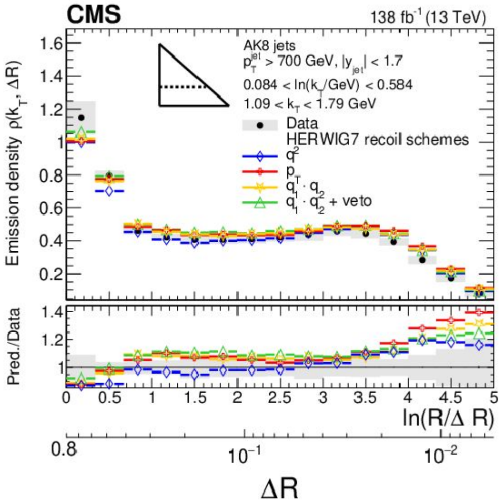

- Better agreement with predictions based on cluster fragmentation models (**HERWIG7** or **SHERPA**)
- **PYTHIA8** overestimate data by 15-20%, regardless of tune or parton shower option

Energy correlators

[CMS-SMP-22-015](CMS-SMP-22-015)

- Multiparticle energy correlators - describe the correlations of kinematic properties of particles within a jet

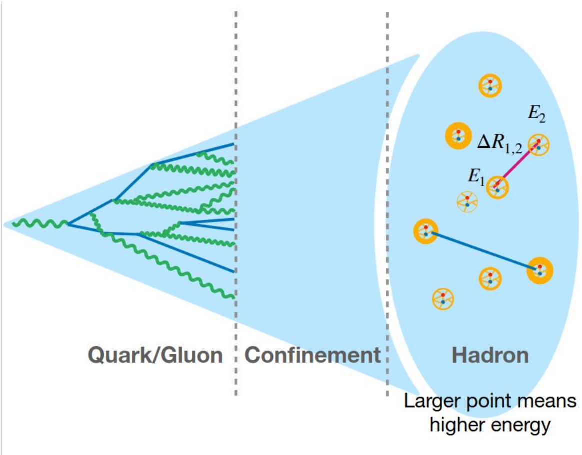

➢ Measurement of two- and three-particle energy correlators

$$E2C = \sum_{i,j}^{3} \int d\sigma \frac{E_i E_j}{E^2} \delta(x_L - \Delta R_{i,j})$$

$$E3C = \sum_{i,j,k}^{3} \int d\sigma \frac{E_i E_j E_k}{E^3} \delta(x_L - max(\Delta R_{i,j}, \Delta R_{i,k}, \Delta R_{j,k}))$$

- x_L - largest distance $\Delta Ri,j$ between constituents

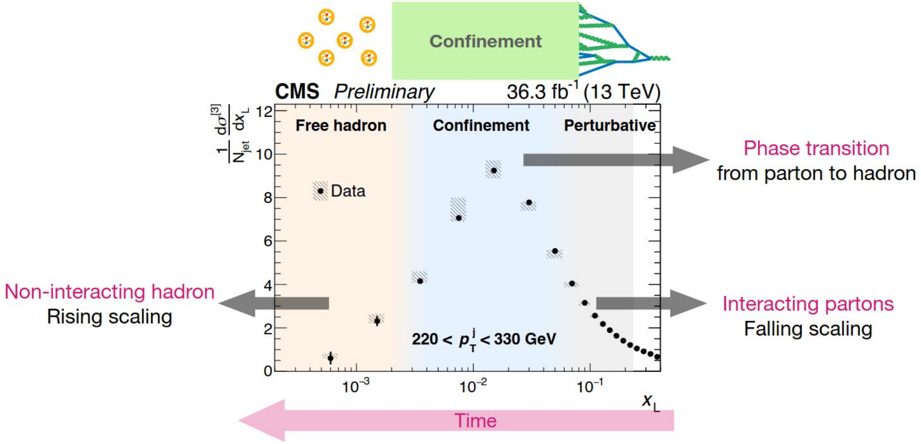

- Mapping out different stages of jet formation:
  → small angle x_L dominated by hadronization
  → large x_L dominated by short distance physics)

Energy correlators

CMS-SMP-22-015

- pp data collected at $\sqrt{s}$ = 13 TeV , integrated luminosity of 36.3 fb^{-1}
- At least two jets anti-k_T, with $|\eta|<2.1$, binned in jet p_T in 97 ~ 1784 GeV
- Using all particles in the jet with p_T > 1 GeV
- Distributions unfolded to particle level

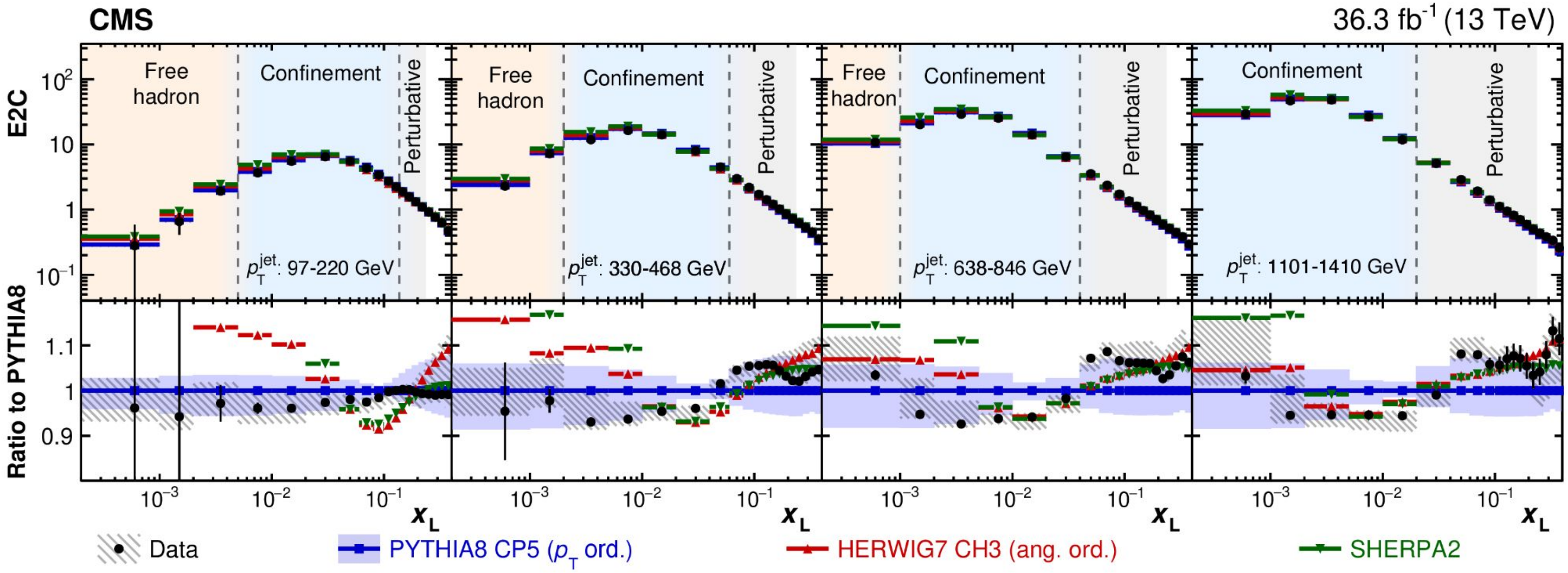

Energy correlators

CMS-SMP-22-015

- Ratio between the E3C and E2C x_L distributions - used to extract the α_S value with good precision
- Theoretical predictions of the ratio at NLO + NNLLapprox
- Comparison of measured E3C/E2C as a function of x_L with the corresponding theoretical predictions - fit χ^2 value as a function of α_S (m_Z)

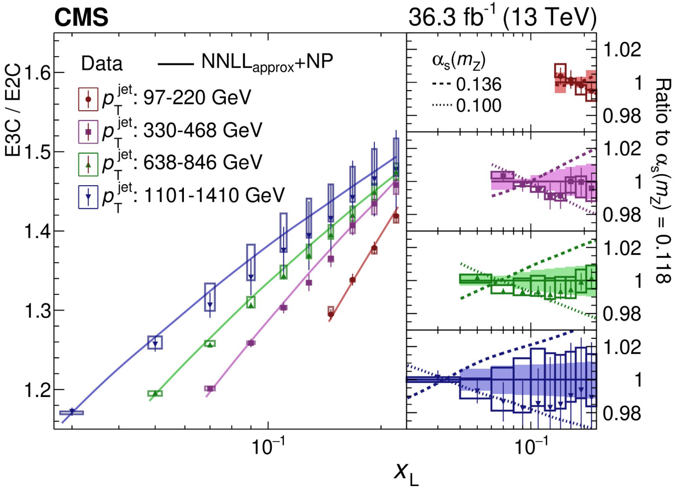

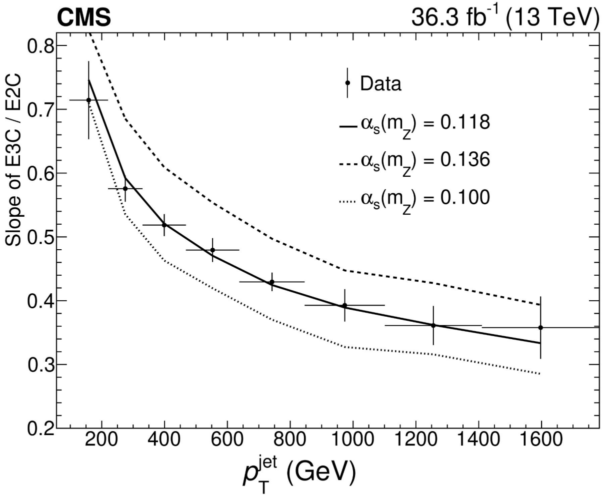

$$\alpha_S(m_Z) = 0.1229^{+0.0040}_{-0.0050}$$

Most precise extraction of α_s *(mZ)* with jet substructure

Long-range elliptic anisotropies inside high-multiplicity jets

CMS-HIN-21-013

- Extreme parton densities in heavy ion collisions - strong partonic rescatterings, **long-range collective flow effects**
- Long-range collective correlations - azimuthal distributions of pp collision events with large final-state particle multiplicity

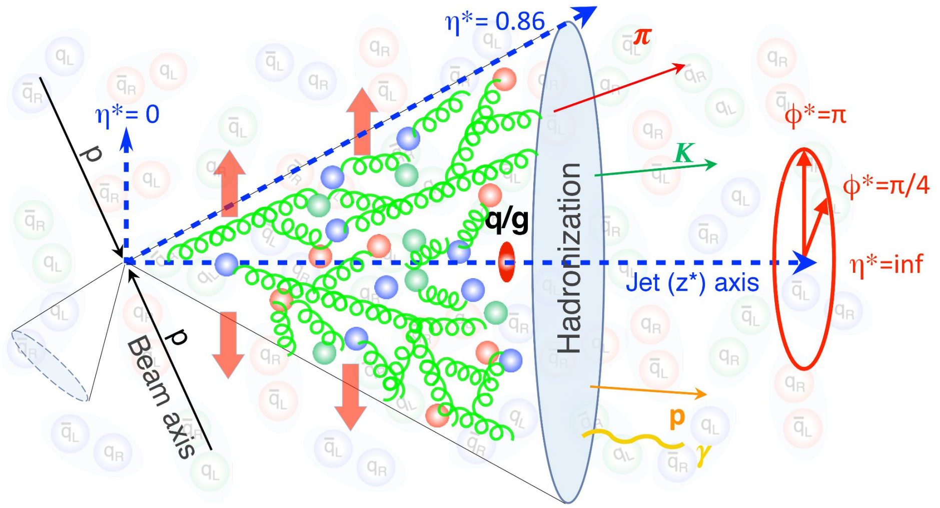

- Collective effects can emerge from an initial system as small as an energetic parton that fragments and hadronizes in the vacuum
- Sufficiently large number of rescatterings during the fragmentation that produces a very high multiplicity jet - lead to a **flow-like behavior similar to that seen in QGP**

Long-range elliptic anisotropies inside high-multiplicity jets

[CMS-HIN-21-013](CMS-HIN-21-013)

- Search for partonic collective effects inside jets produced in pp collisions
- Data collected at $\sqrt{s}$ = 13 TeV, integrated luminosity of 138 fb^{-1}
- Anti-k_T jets with distance parameter R= 0.8, p_T > 550 GeV, $|\eta|$ < 1.6

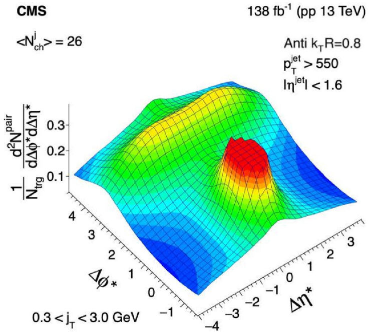

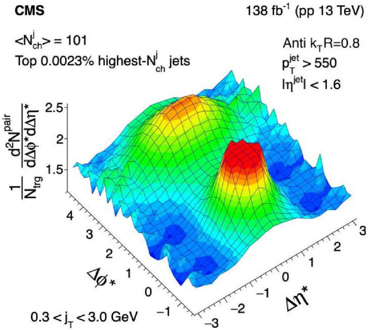

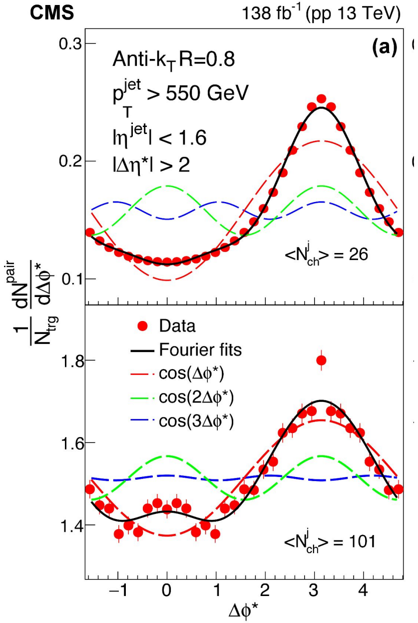

- Two-particle correlations among the charged constituents - as functions of the $\Delta\phi^*$ and $\Delta\eta^*$

$\eta*$, $\phi*$ - azimuthal angle and pseudorapidity defined relative to the direction of the jet

⇒ **Indication of a near-side ridge in the high-N^j_{ch}**

Long-range elliptic anisotropies inside high-multiplicity jets

CMS-HIN-21-013

- Two-particle Fourier coefficients for the first three harmonics $V^*_{n\Delta}$ as a function of $\langle N_{ch}^{j} \rangle$

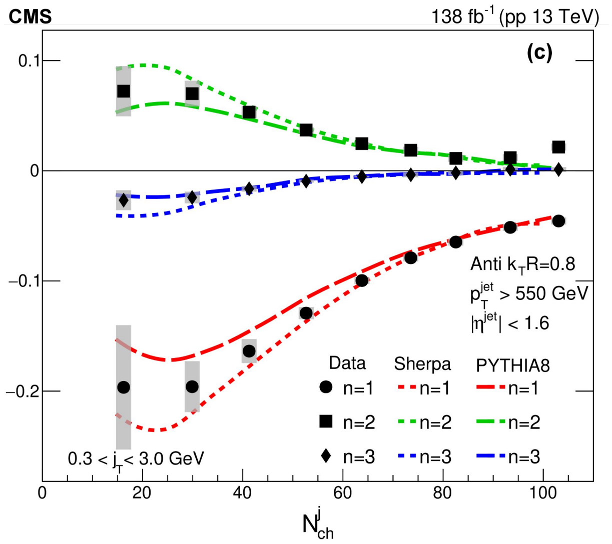

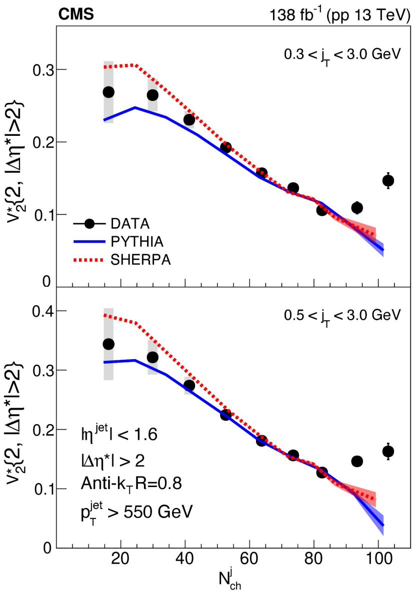

- Odd-order harmonics, $V^*_{1\Delta}$ and $V^*_{3\Delta}$ negative, $V^*_{2\Delta}$ positive over full range
- The magnitudes of all harmonics tend to decrease as $\langle N^{j}_{ch} \rangle$ increase

➢ Single-particle elliptic anisotropies - data start to show a steady increases with for $N^{j}_{ch} > 80$ not observed in either **PYTHIA 8** or **SHERPA**

⇒ **possible onset of collective behavior**

Groomed jet radius and girth of jets recoiling against isolated photons

CMS-PAS-HIN-23-001

- Heavy-ion collisions - production of high-temperature, strongly interacting phase of nuclear matter
  Quark Gluon Plasma (QGP)
- Degradation the jet energy and modification of the jet radiation pattern due to the interaction with medium - **jet quenching**

sketches by Ray Cruz

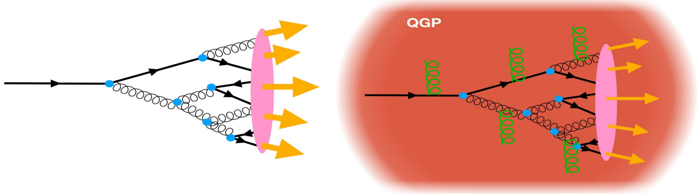

pp ("vacuum") *PbPb ("medium")*

- Main interaction mechanism between the jet constituents and the medium at short distance scales - **medium-induced radiation**

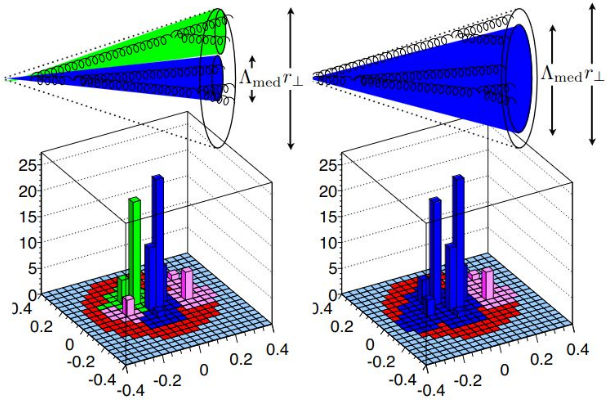

➢ The medium resolution length - angular separation between two partons or subjets below which the medium cannot resolve them as independent color charge

⇒ more resolved constituents - interact more with the medium and be more quenched

Groomed jet radius and girth of jets recoiling against isolated photons

CMS-PAS-HIN-23-001

- **Groomed jet radius Rg** - the angle between the two subjets selected by the soft drop grooming algorithm
- **Jet girth** - sum of the product of the momentum fraction of the jet constituents and their distance relative to the anti-k_T jet axis

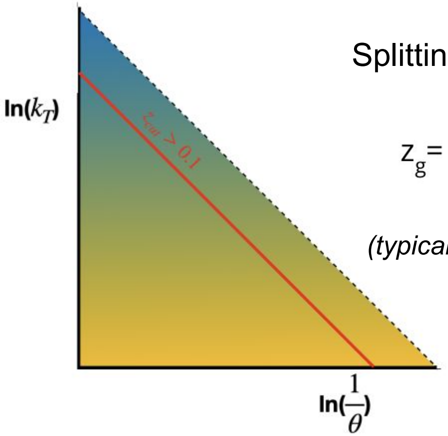

Splittings selected by Soft drop algorithm:

$$z_g = \frac{\min(p_T^{(1)}, p_T^{(2)})}{p_T^{(1)} + p_T^{(2)}} > z_{cut} \left(\frac{\Delta R_{12}}{R} \right)^{\beta_{sd}}$$

(typical choice in heavy-ions is β_{SD} = 0, z_{cut} = 0.2)

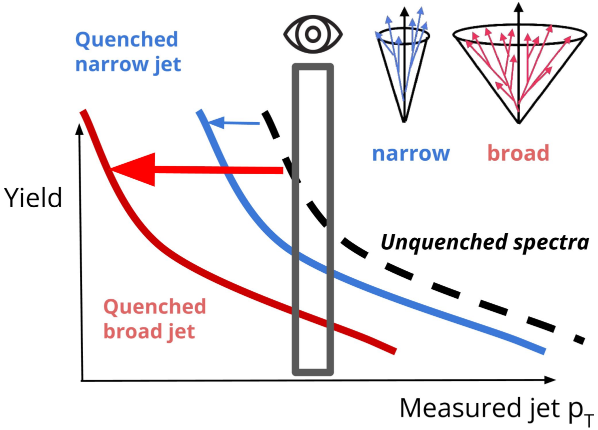

- selection bias that emerges when comparing pp and PbPb jets with the same reconstructed p_T

⇒ **Photon does not interact strongly with the QGP - proxy for the unquenched p_T^{jet}**

Two categories for measurement:

- p_T^{jet}/p_T^{photon} > 0.4 (quenched and nonquenched jets)
- p_T^{jet}/p_T^{photon} > 0.8 (less quenched jets)

Groomed jet radius and girth of jets recoiling against isolated photons

CMS-PAS-HIN-23-001

- pp and PbPb data collected by the CMS 2017 and 2018, respectively at a nucleonnucleon center-of-mass energy of 5.02 TeV integrated luminosities of 301 pb^{-1} and 1.7 nb^{-1}
- The distributions are unfolded to the level of stable particles

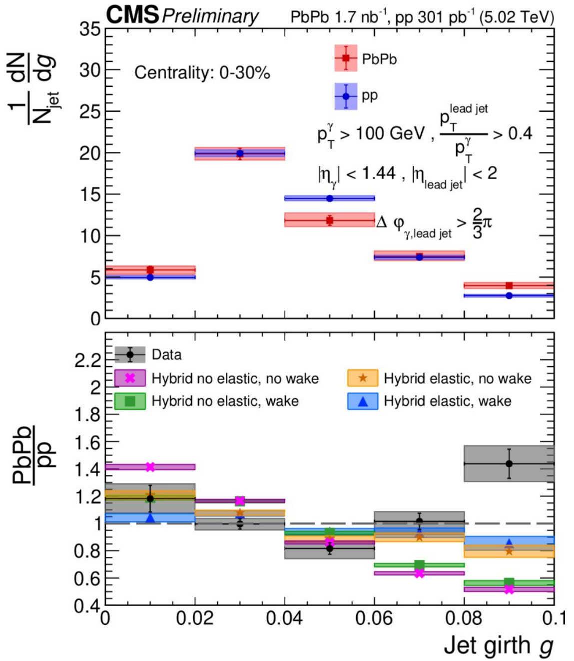

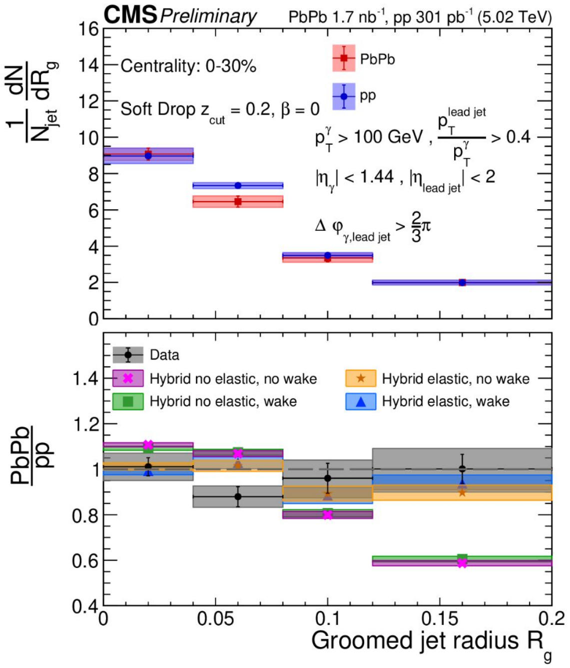

➢ Both quenched and less quenched jets selected - no narrowing of the angular structure

- **The Hybrid predictions with elastic scatterings** describe the data better than the predictions without elastic scatterings

Elastic *- energy loss due to the strong coupling between the partons and the medium*
Wake *- the nonperturbative backreaction of the medium*

Groomed jet radius and girth of jets recoiling against isolated photons

[CMS-PAS-HIN-23-001](CMS-PAS-HIN-23-001)

- pp and PbPb data collected by the CMS 2017 and 2018, respectively at a nucleonnucleon center-of-mass energy of 5.02 TeV integrated luminosities of 301 pb^{-1} and 1.7 nb^{-1}
- The distributions are unfolded to the level of stable particles

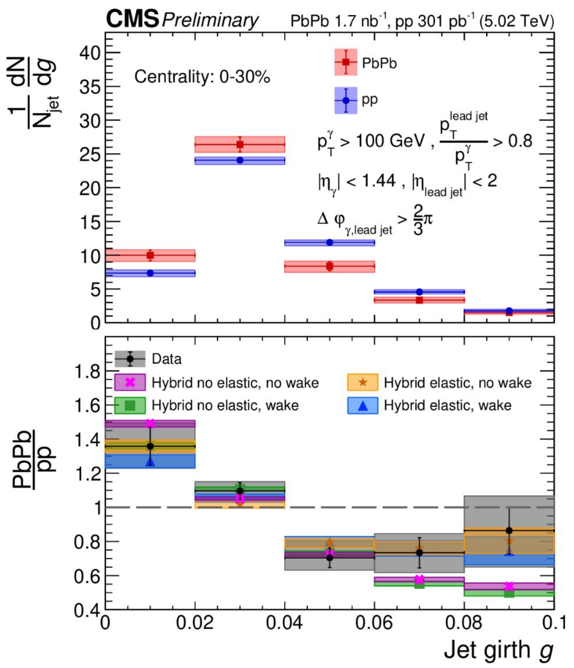

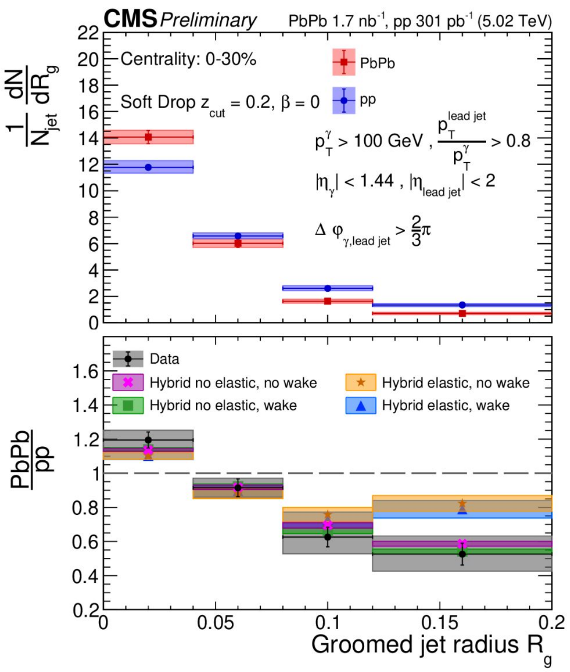

➢ Less quenched jets selected - narrowing of the angular structure

- **The Hybrid predictions with no elastic scatterings** describe the data better than the prediction with elastic scatterings

Elastic *- energy loss due to the strong coupling between the partons and the medium*
Wake *- the nonperturbative backreaction of the medium*

Summary

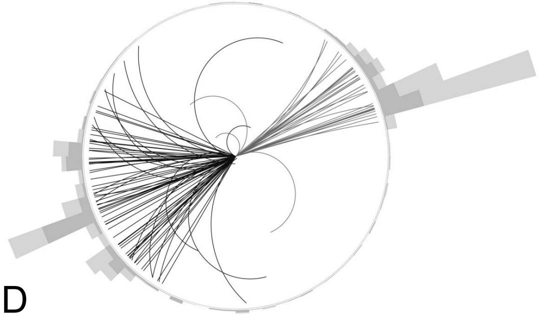

- Measurements of jet substructure expose the basic building blocks of QCD
- These measurements can be used to improve different aspects of the physics modeling in event generators
- Jet substructure can be used to extract α_S
- Collective behavior studies - new insights into the dynamics of parton fragmentation processes in the vacuum
- Photon tagged jets - better controlled assessment of the modification of the angular scale of jets and of sensitivity to microscopic properties of the QGP